OPEN

Correspondence and
requests for materials
should be addressed to
M.P.S. (ms2001@
columbia.edu) or J.Y.
(phyyj@nus.edu.sg)

* These authors
contributed equally to
this work.

Mechanical activation of vinculin binding to talin locks talin in an unfolded conformation

Mingxi Yao[1]*, Benjamin T. Goult[2]*, Hu Chen[1,3], Peiwen Cong[1,4], Michael P. Sheetz[1,5] & Jie Yan[1,6,7]

[1]Mechanobiology Institute, National University of Singapore, 117411, Singapore, [2]Department of Biochemistry, University of Leicester, Henry Wellcome Building, Leicester, LE1 9HN, UK, [3]Department of Physics, Xiamen University, Xiamen, Fujian, 361005, China, [4]Singapore-MIT Alliance for Research and Technology, National University of Singapore, 117543, Singapore, [5]Department of Biological Sciences, Columbia University, New York, NY 10027, USA, [6]Department of Physics, National University of Singapore, 117542, Singapore, [7]Centre for Bioimaging Sciences, National University of Singapore, 117546, Singapore.

The force-dependent interaction between talin and vinculin plays a crucial role in the initiation and growth of focal adhesions. Here we use magnetic tweezers to characterise the mechano-sensitive compact N-terminal region of the talin rod, and show that the three helical bundles R1–R3 in this region unfold in three distinct steps consistent with the domains unfolding independently. Mechanical stretching of talin R1–R3 enhances its binding to vinculin and vinculin binding inhibits talin refolding after force is released. Mutations that stabilize R3 identify it as the initial mechano-sensing domain in talin, unfolding at ~5 pN, suggesting that 5 pN is the force threshold for vinculin binding and adhesion progression.

Mechanical forces can regulate biochemical changes important for cell survival, growth, and migration[1]. One type of force-dependent regulation is achieved by mechanosensitive protein-protein interactions, and such interactions play an important role in the formation of integrin-containing adhesions which control cell migration on the extracellular matrix (ECM)[2]. The mechanosensitive protein talin binds integrins, increases their affinity for ECM and couples them to cytoskeletal actin leading to formation of small nascent adhesions at the leading edge of migrating cells. Force exerted on nascent adhesions leads to recruitment of vinculin which binds talin via a force-dependent mechanism, and this plays a crucial role in the regulation of focal adhesion (FA) initiation and growth[3–6].

Talin comprises an N-terminal FERM domain (50 kDa) that binds integrin cytodomains and acidic membrane phospholipids synergistically[7,8]. The C-terminal talin rod (220 kDa) contains 13 helical bundles (R1–R13) terminating in a single helix that supports talin dimerisation (Fig 1a)[9]. It contains eleven putative vinculin binding sites (VBS), each defined by hydrophobic residues on a single helix, but these are normally buried within the helical bundles[10]. The talin-vinculin interaction occurs primarily through the association of the vinculin head (Vd1) domain with these VBS[11,12]. Steered full-atom molecular dynamics (MD) simulations indicate that the cryptic VBS may be exposed by mechanical force resulting from actomyosin contractions *in vivo*[13,14]. This hypothesis is supported by experiments that revealed substantial increases in the vinculin-talin interaction when talin was subjected to forces of ~12 pN with magnetic tweezers[15]. However, in this previous study the conformational changes of talin at <20 pN were not measured. Therefore, neither the forces required to initiate vinculin binding nor the force-dependent talin conformations necessary to facilitate vinculin binding are known. Our recent completion of the domain structure of talin[9] identified that the N-terminal compact region of the rod, R1–R3, is most likely to change conformation in response to mechanical force due to its more compact arrangement.

Talin rod domains can exist in three structurally distinct conformations under force (Fig 1b): (i) Folded α-helix bundles under low forces, where the VBS are buried and inaccessible. (ii) An extended chain of α-helices, where the VBS are exposed under intermediate force. (iii) A fully unfolded polypeptide chain under high forces. Prior to this work the forces at which these conformations occur and how they are coupled to vinculin binding have not been investigated. In this work, we examined the stability of vinculin Vd1 binding to the talin R1–R3 rod domains across a wide range of force (0.5–50 pN) and Vd1 concentrations (0.1–100 nM) and show that this region is mechanically sensitive. This study advances our understanding of the mechanosensitive interaction between talin and vinculin and identifies the initial vinculin attachment site as being the R3 rod domain which has significant implications for adhesion assembly and progression.
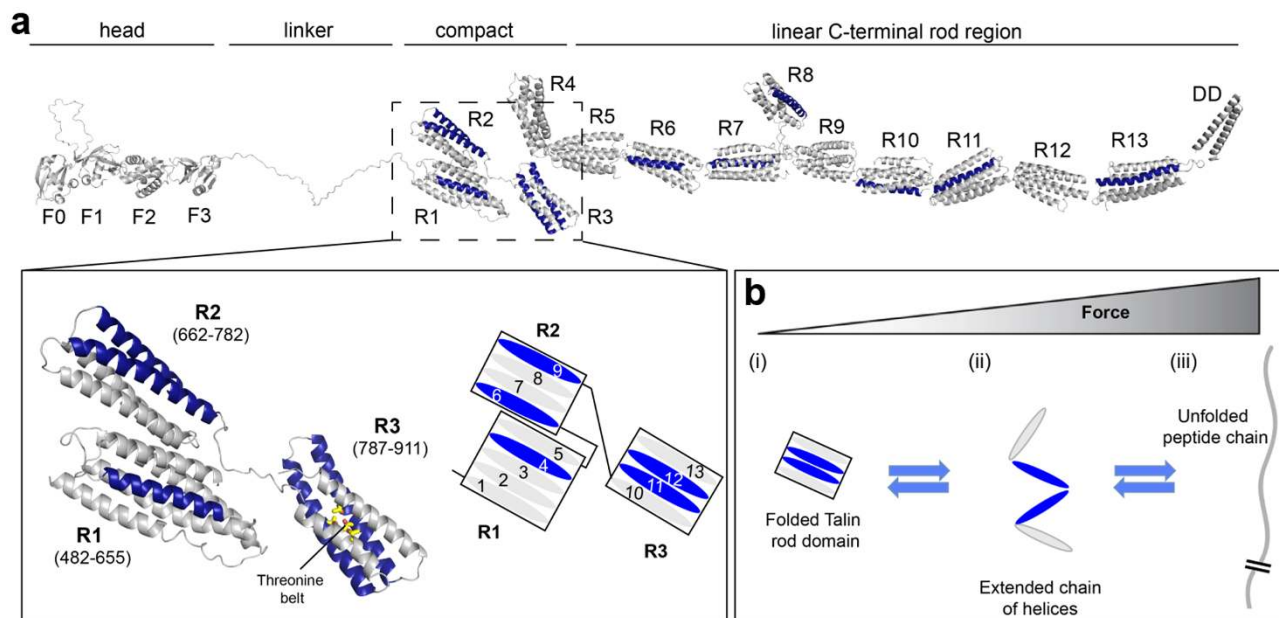
Figure 1 | Structural model of full-length talin. (a) Talin is comprised of a FERM domain containing Head joined by a large unstructured linker to a flexible rod comprised of thirteen 4- or 5- helix bundles (R1–R13). The talin rod has two distinct regions, a compact N-terminal region (R1–R3) and a linear C-terminal region (R4–R13). Putative vinculin binding sites are shown in blue. (Inset) Schematic representation of the compact region of the talin rod studied in this work. The threonine belt that destabilizes the R3 domain is highlighted. (b) Schematic of three possible force-dependent conformations of a talin rod domain.

Results

Talin R1–R3 unfolds in three characteristic steps. The recent structural characterization of full-length talin[9] (Fig 1a) shows that the talin rod is comprised of 13 helical bundles (R1–R13) organized into two distinct regions, a compact N-terminus comprising R1 to R3 (residues 482–911) likely to change conformation in response to force, attached to a long linear rod region encompassing 10 further bundles, R4–R13 (residues 913–2482) perfectly suited to force transmission. The compact N-terminal region of the talin rod (R1–R3) is atypical as both R2 and R3 each contain two VBS[9].

Our previous studies on the talin fragment 482–889 using atomic force microscopy (AFM) showed that this region undergoes force-dependent conformational changes at >20 pN[15]. However, several important questions remained unanswered, such as whether lower, more physiologically relevant, forces can cause conformational changes and whether such changes can be reversed. Further, although talin 482–889 contained most of the compact N-terminal region of the rod, the fourth helix of the R3 domain (helix 13) was missing. Therefore, we wanted to characterize the force responses of the complete N-terminal region, R1–R3 (482–911) containing the intact R3 domain. To characterize the force-dependent conformations we mechanically stretched R1–R3 using magnetic tweezers (Fig 2a–b). We performed force cycling experiments that consist of a force-increase step followed by a force-decrease step. In the force-increase step, force was increased linearly with time at a constant loading rate until the talin rod was fully unfolded. In the subsequent force-decrease step, force was decreased exponentially with time until a force of 0.5 pN was reached. At 0.5 pN, the tether was held for 1 minute to allow refolding of the talin domains.

At a loading rate of 5 pN/s in the force-increase procedure, we found that R1–R3 began to unfold at ~5 pN and was completely unfolded at ~25 pN (Fig 2b). Strikingly, the completely unfolded talin rod fragment refolded within one minute at 0.5 pN (Fig S1a–b). Additionally, we reproducibly observed three major unfolding steps (Fig 2b) during each subsequent force-increase procedure after talin rod refolding, which were distinct in both unfolding forces and step

sizes. These distinct unfolding steps were observed in >10 independent experiments using different talin rod tethers (Fig S1a–b).

Interestingly, equilibrium unfolding/refolding fluctuations were observed when the talin rod fragment was held at constant forces near 5 pN (Fig S2) suggesting that the initial unfolding event is dynamic, and can readily refold in the absence of other factors.

Our results suggest that each domain in R1–R3 has a unique response to mechanical force with the three unfolding steps most likely corresponding to unfolding of the three rod-domains. In particular, one rod domain has a striking susceptibility to unfolding in response to weak mechanical forces of ~5 pN.

The talin R3 domain unfolds at lowest force. Our previous biochemical analysis of talin identified four threonine residues buried in the hydrophobic core of R3 (Fig 1a) that destabilize the bundle, suggesting that R3 is likely to be the first to recruit vinculin in response to the initial weak forces exerted on nascent adhesions[9]. Mutation of these threonines to hydrophobic valine and isoleucine residues (T809I/T833V/T867V/T901I; the IVVI mutant, Fig 1a) markedly stabilized the bundle with minimal effects on its overall structure[9]. Furthermore, this increase in domain stability had a dramatic effect on vinculin binding to R1–R3, requiring incubation at higher temperatures to bind vinculin. To directly test the hypothesis that R3 provides the initial site for vinculin recruitment in response to the initial weak forces, we investigated the force response of the R1–R3 IVVI mutant and compared it with wild-type (WT) R1–R3.

The unfolding profile of the R1–R3 IVVI mutant stretched at 5 pN/s was similar to that observed for the WT R1–R3 in that we observed three discrete unfolding steps (Fig 2b–c). However, whilst the two peaks at higher forces remain comparable to WT R1–R3 the peak that unfolds at lowest force shifted from ~5 pN to ~8 pN, which is significantly greater than our <15% relative errors in force calibrations[16].

This suggests that the unfolding observed at 5 pN corresponds to the talin R3 domain and confirms R3 as the initial mechano-sensing domain in the compact N-terminal region of talin.
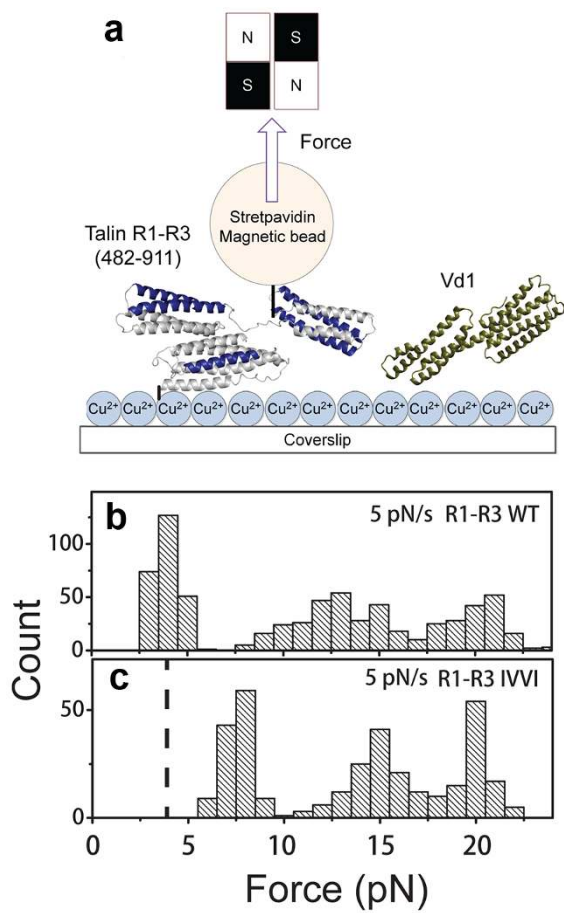
Figure 2 | Stretching single talin rod molecules. (a) Schematic of experimental setup. A talin rod construct is tethered between a cover glass surface and a paramagnetic bead through NTA-His tag and streptavidin-biotin linkages. Force is applied to the paramagnetic beads using a pair of permanent magnets. Talin rod constructs are stretched in the presence or absence of vinculin Vd1. (b–c) The unfolding force distribution histograms of wild type talin R1–R3 (b) and threonine belt IVVI mutant (c) when stretched at a constant loading rate of 5 pN/s.

Vinculin head binds to the unfolded talin rod and inhibits domain refolding. Overexpression of the vinculin head domain, Vd1, *in vivo* leads to elongation of talin[11]. However, it is unclear whether this elongation is due to direct binding of Vd1 to talin, and we therefore sought to examine how Vd1 interacts with talin. In the absence of Vd1, talin R1–R3 shows three discrete unfolding events during each force increase scan (Fig 3a). To determine whether talin rod unfolding requires force or can be induced by Vd1, we repeated this experiment in the presence of 10 nM Vd1. We found that talin R1–R3 remained folded at low force, until higher forces were applied where we observed three discrete unfolding events (Fig 3b) similar to that observed in the absence of Vd1 (Fig 3a). However, after the talin rod was unfolded in the first force-increase scan, unfolding events were not observed in subsequent force cycles. This Vd1-dependent decrease in talin rod unfolding frequency can be explained by Vd1 binding to mechanically exposed VBS. In this scenario, association of exposed VBS with Vd1 inhibits talin rod refolding at low force. Therefore, in the next force-increase scan, the bundle is already unfolded (and bound to vinculin), and as such, the corresponding unfolding step is absent. These results indicate that mechanical stretching, rather than vinculin head concentration triggers the unfolding of the talin rod and that once bound, Vd1 inhibits talin rod refolding at low forces.

To further examine how Vd1 binds to the mechanically unfolded talin rod and to determine how bound Vd1 affects refolding of the talin rod at low forces, we repeated the force cycling experiment in the presence of 1 nM Vd1. Under these conditions, we found that the overall frequency of the unfolding events was reduced (Fig 3c and e). Additionally, we found that at a higher concentration of Vd1 (10 nM), the frequency of unfolding at >15 pN forces was reduced by >90%, although some unfolding events were still observed at low forces (Fig 3d and e). These residual unfolding events occurs at similar force to the initial unfolding event in R1–R3 when R3 unfolds at ∼5 pN (Fig. 2b). To see whether this suggests that unfolded R3 could refold in the presence of Vd1, we performed a force cycle experiment across a low force range (1–7 pN) over which only R3 would be expected to unfold. In the absence of vinculin the unfolding step corresponding to R3 is clearly visible in each cycle (Fig 3f). However, upon addition of 10 nM Vd1 the unfolding step is lost in all subsequent cycles confirming that Vd1 can bind to the unfolded R3 at <7 pN force and remains bound across this force range. Furthermore, the residual unfolding events at low forces in Fig 3d and e were not observed. This indicates that upon unfolding all three domains are bound to vinculin and the residual unfolding events observed at low forces in Fig 3e are likely due to weak associations of some exposed talin helices in the completely unfolded R1–R3.

The fact that we observe an inhibitory effect on talin rod refolding at Vd1 concentrations as low as 1 nM, suggests high affinity Vd1 binding to exposed VBS in the nM range of the dissociation constant (K_d) although it is striking that we do not observe Vd1 binding in the absence of force. This high binding affinity may be relevant to the ability of the talin rod to activate vinculin by competing off the auto-inhibited head to tail association of full-length vinculin[17].

In addition, we found that at low force, the talin rod extension was higher in the presence of Vd1, at both 1 and 10 nM concentrations, than in its absence (Fig 3c–d, f). The longer extension of the talin rod at low force in the presence of Vd1 can be explained by vinculin binding which locks the talin rod in an unfolded conformation.

Overall, multiple talin rod stretch-relaxation cycles in the presence of Vd1 show that stretch exposes otherwise buried VBS in the talin rod. Furthermore, Vd1 binding inhibits the refolding of the talin rod and a force of less than <7 pN is sufficient to initiate this process.

Vinculin head dissociates from talin at >25 pN forces. Vd1 binds to VBS when they are in the α-helix conformation. However, at sufficiently large forces, the α-helices become unstable, which may result in a helix-to-coil transition[18,19]. Therefore, at a sufficiently high force, Vd1 dissociation should occur as the VBS unfolds, accompanied by a small unfolding step due to the extension that occurs during the subsequent VBS helix-to-coil transition. This dissociation force should be higher than the helix-to-coil transition force of the VBS in the absence of bound Vd1, as overcoming the binding energy between Vd1 and the VBS requires additional work. Consistent with these predictions, in the presence of Vd1, small unfolding steps (∼3 nm) were often observed at forces >25 pN (Fig 3c–d). These unfolding step sizes are consistent with the estimated extension increase from helix-to-coil transitions of one VBS at 20–40 pN (see Supplementary Materials and Methods). Furthermore, using a force jump protocol where, at 10 nM Vd1 concentration, a talin rod molecule was unfolded by a large force of ∼40 pN, we can clearly observe vinculin head dissociation events, indicated by the characteristic ∼3 nm unfolding steps (Fig 4a). The frequency of these high-force dissociation events increases with increasing vinculin concentration (Fig 4b) and the typical number of dissociation events detected is 2–3. As R1–R3 contains five VBS this suggests that either not all the VBS are engaged, or the force applied is not sufficient to displace vinculin within the duration of the experiment (5 seconds). However, in a few cases where the
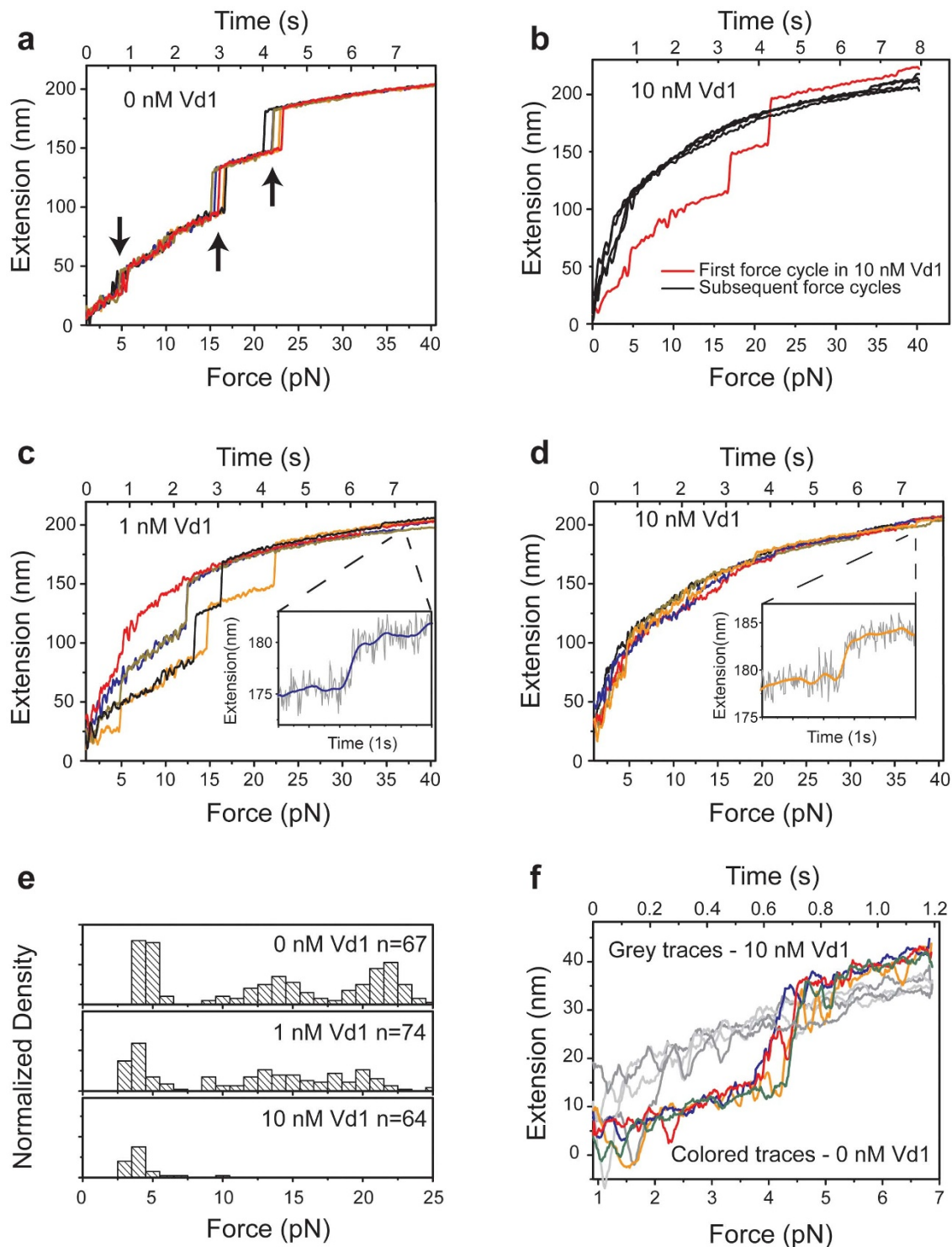
Figure 3 | Effects of vinculin Vd1 on talin rod refolding. (a–b) Vinculin Vd1 does not trigger talin rod unfolding at low forces. Five representative unfolding force-extension curves were selected from >30 repeating stretch-relaxation cycles, at Vd1 concentrations of (a) 0 nM and (b) 10 nM. The curves are smoothed with a 0.05 s time window and the time trajectories of the extension change during multiple force-increase scans at a constant loading rate of 5 pN/s are shown in the top x axis. In each force-increase scan, time zero is set to be the beginning of the force scan; therefore curves from different scans can be plotted in one figure panel. (a) In the absence of Vd1, the curve shows three unfolding events during the stretch phase in each cycle. (b) After incubation with Vd1, the characteristic unfolding steps were observed in the first force-cycle stretching (red). Unfolding events were absent in subsequent force-cycles (black), indicating complete inhibition of talin rod refolding by Vd1 bound to mechanically exposed VBS in the first force-increase scan. (c–d) The effect of lower Vd1 concentrations (a) 0 nM (c) 1 nM and (d) 10 nM. For clarity the initial unfolding curve is omitted. Insets in (c) and (d) show ~3 nm steps consistent with force-induced vinculin head dissociation at high forces (see explanation in main text). (e) Histogram of talin rod unfolding forces at different Vd1 concentrations obtained from two independent talin rod tethers, normalized by the number of stretch-relaxation force cycles. (f) R3 can be activated for Vd1 binding at less than 7 pN of force. Force cycle experiments between 1 and 7 pN for a single WT R1–R3 tether in the absence (colored traces) or in the presence (grey traces) of 10 nM Vd1.
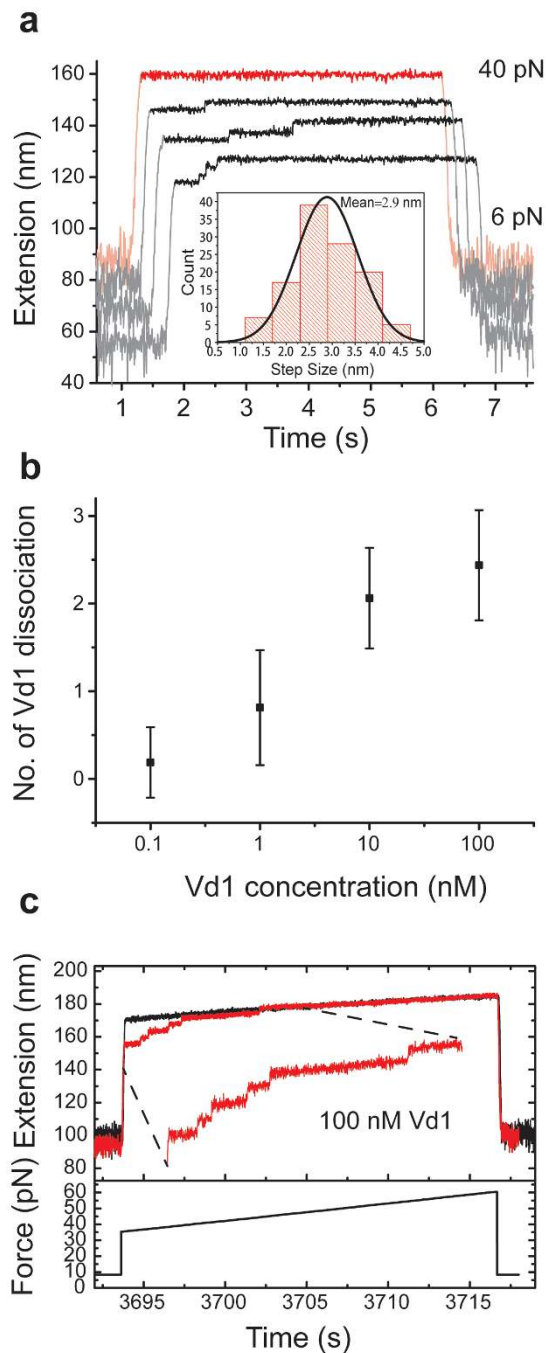
Figure 4 | Vinculin Vd1 dissociates from talin at high force. (a) Time-lapse data of talin rod in 0 nM (red) and 10 nM (black) of Vd1 during force jumping between 6 pN for 1 min, during which no domain refolding was observed (pink/grey), and 40 pN for 5 s (red/black). For clarity, the curves are shifted along the extension-axis to avoid overlapping. Inset shows histogram of the unfolding step sizes at 40 pN. (b) Number of Vd1 dissociation events observed with the same procedure as in (a) as a function of Vd1 concentration. Error bar denotes standard deviation. (c) Maximally five Vd1 dissociation events have been observed in rare cases with strong tethers when stretched from 35 pN to 60 pN at a constant loading rate of 1 pN/s.

attachment of the protein to the cover slip was strong enough to withstand higher forces (Fig 4c), up to five dissociation events were observed by ~50 pN consistent with maximal vinculin binding. Taken together, these results indicate that Vd1 binding to exposed VBS can be reversed at large forces.

Discussion

In this study we have characterized the force-dependent interaction between the vinculin head and the compact N-terminal region of the talin rod. Previous studies have shown that stretching talin molecules activates vinculin binding[5,6,15]. Furthermore, recent elegant studies using *in vitro* reconstitution of actomyosin cables - FL-talin interactions on micropatterned surfaces have clearly demonstrated that the forces exerted on talin by actomyosin contraction are sufficient to recruit vinculin in a reversible manner[6].

However, these studies did not elucidate how different force-dependent talin rod conformations bind Vd1 nor the force required for vinculin binding. Here we take advantage of the recently determined structures of the talin rod[9] and advancement of magnetic tweezers technology to define, for the first time, the precise mechanisms by which the compact N-terminal region of the talin rod (domains R1–R3) interacts with vinculin in a force dependent manner. Our results indicate that a differential force response of talin R1–R3 determines the level of vinculin binding in a force dependent manner (Fig 2–3). We show that R1–R3 displays three major unfolding steps, occurring at different forces in the range of 5–25 pN, and corresponding to the three domains unfolding (Fig 2b). All three unfolding events expose VBS buried in each of the talin rod domains (Fig 1a and Fig 3). Furthermore, we identify the talin rod unfolding step observed at low force, ~5 pN, as pertaining to the R3 rod domain since mutating the destabilizing "threonine belt", a unique feature of R3, via an IVVI substitution[9] shifts the initial unfolding step (Fig 2b). This is the first time that the R3 domain has been identified as the initial mechano-sensor in talin, and provides unique insight into adhesion regulation.

Our results suggest that vinculin head binding is biphasic, inhibited by two force regimes: in the small force range (<5 pN) where the talin domains exist as folded helical bundles, and a high force range (>25 pN) where the bound vinculin heads are displaced from the talin rod by helix-to-coil transitions. The low force regime is likely present during early focal adhesion formation with low myosin activity. Similarly, the higher forces required to unfold α-helices can be generated *in vivo* by small focal adhesions, since single actin filaments associated with focal adhesions can support forces of >100 pN[20]. Thus, talin rod binding of vinculin may be biphasic *in vivo*. In addition to providing a comprehensive description of the force-dependent talin rod conformations over physiological force ranges, these results also provide a general framework to understand the force-dependent manner by which binding partners access the buried binding sites in the talin rod domain. By directly comparing wild-type with the IVVI R3 mutant, we have demonstrated that it is possible to assign unfolding events to individual talin rod domains.

Surface Plasmon Resonance studies of vinculin head binding to isolated talin VBS peptide reveal that this interaction has a high affinity, with a dissociation constant $K_d \sim 2$ nM[17,21]. Our results demonstrate that the vinculin head domain binds to mechanically exposed VBS in the talin rod domain with comparable affinity (Fig 3c). This strong interaction between Vd1 and mechanically stretched talin may be important for vinculin activation by competing off the vinculin head-to-tail association of auto-inhibited vinculin. Further, we found that vinculin-binding inhibits refolding of the talin rod molecule upon the release of force. These results may explain the recent *in vivo* observation that overexpression of Vd1 leads to stable elongation of full-length talin near focal adhesion sites of cells[11]. The stable association between Vd1 and talin VBS helices may provide a signaling mechanism that is robust to force fluctuation.

Overall, our results provide important insights into *in vivo* talin functions. We reason that a positive feedback mechanism may exist to reinforce stress fiber formation at focal adhesions. Our results are consistent with a model whereby at ~5 pN force, which is the force exerted by a single myosin molecule *in vivo*, initial binding of Vd1 to the least stable talin rod domain, R3, may occur (Fig 5). This may, in
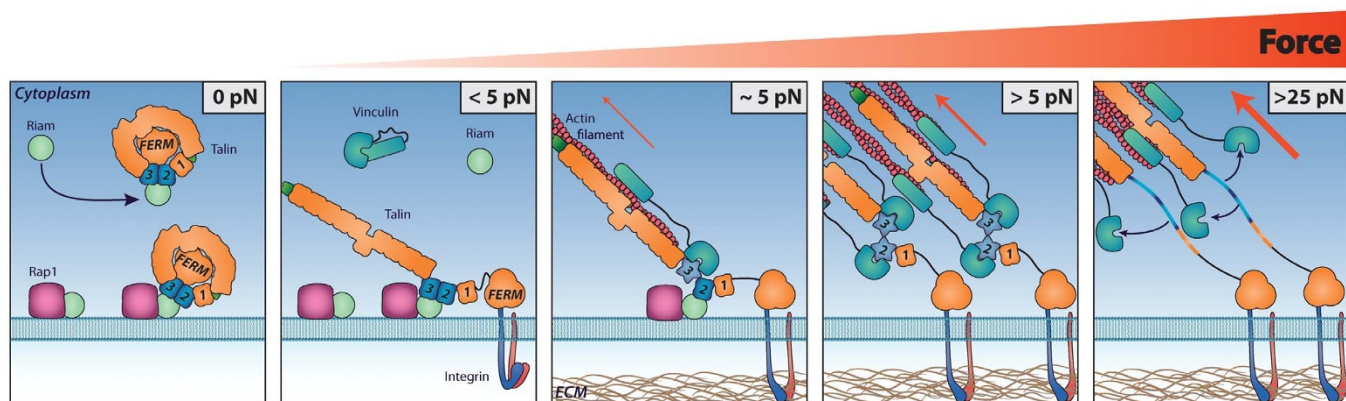
5

Force

Figure 5 | Talin changes binding partners in response to force induced conformational change. Force plays a key role in driving the formation of FA. **0–5 pN**: RIAM recruits autoinhibited talin to the plasma membrane in a Rap1.GTP dependent manner via synergistic binding of RIAM to the R2–R3 domains of talin. At the membrane talin autoinhibition is relieved by interactions with acidic membrane phospholipids. Talin can then activate integrins. **~5 pN**: Only when talin has engaged the integrins and also captured the retrograde flow of actin is force exerted on talin. At ~5 pN, the force of a single actomyosin contraction, the R3 domain is destabilized and this reduces RIAM binding whilst exposing the high affinity VBS which then bind vinculin strengthening the adhesion. **>5 pN**: With more vinculin cross-linking the adhesion can withstand greater force exposing further VBS. **>25 pN**: At sufficiently high forces vinculin is displaced, resulting in unfolding of the VBS to a random coil.

turn, lead to a low level of vinculin activation, stabilizing the initial talin/actin linkage within the nascent adhesions[9]. Following these initial steps, newly linked actin fibers may result in further increases in force applied to talin, exposing more vinculin binding sites and, ultimately, promoting formation of a stronger actin linkage and the assembly of larger more stable focal adhesions.

This fits with a model where only when the talin starts to engage the β-integrin tail and acidic membrane phospholipids via its N-terminal head domain[7,8] and captures the retrograde flow of actin filaments at the leading edge via its C-terminal actin binding site[22,23], will the talin rod experience the tension required to expose its vinculin binding sites (Fig 5). Prior to engagement at the membrane, the talin molecule will experience only very small (<5 pN) forces, and as such, no vinculin binding sites are exposed. At a force of just ~5 pN, the force of a single actomyosin contraction, the R3 rod domain will start to unfold, exposing its two VBS, and vinculin can then bind and cross link talin to actin such that greater forces can be applied. As the force increases, additional vinculin binding sites become exposed increasing the number of vinculin molecules bound to talin, further strengthening its connection to actin. Vinculin also prevents talin refolding which serves as a ratchet possibly preventing inadvertent talin refolding at adhesion onset.

R3 unfolding also has implications for the interaction of talin with the Rap1 effector RIAM, which translocates talin to the membrane[24–26] in an autoinhibited conformation[27–29]. At the membrane talin unfolds, possibly via interaction with PIP2[30] to reveal the active form of talin which then binds and activates integrins. Interestingly, RIAM binds synergistically and with high affinity to the folded R2R3 talin rod domains[9], and here we show that a relatively low force, just 5 pN, is sufficient to unfold the R3 domain which would be predicted to destroy the high affinity RIAM binding site whilst simultaneously exposing the initial high affinity vinculin binding sites in R3. Our data suggest that at <5 pN of force, RIAM binding to talin R2R3 would predominate, supporting integrin activation and the assembly of nascent adhesions, but at around ~5 pN there is a transition to vinculin:talin complexes which drives the maturation of nascent adhesions into focal adhesions. This requirement for force to reveal the vinculin binding sites prevents talin, via its interaction with vinculin, crosslinking to actin randomly in the cell; i.e. force is only exerted on talin when it is engaged with both the integrin and actin which serves as an important checkpoint. Successful adhesion formation requires the clustering of adhesion proteins and it is tempting to speculate that the biphasic force dependence of vinculin

binding to talin may serve as a safety mechanism to ensure this; a single talin molecule in isolation will rapidly experience the high forces where vinculin is displaced, however, if other talin molecules (coupled to other integrin and FA proteins) get recruited the high forces will be distributed such that this 25 pN threshold is not crossed by any single talin molecule and the adhesion can develop. Hence the biphasic nature of vinculin binding to talin may have potential to serve as a positive reinforcement of clustering.

The results from this work indicate that vinculin binds to cell-matrix adhesions through the mechanical exposure of buried vinculin binding α-helices in talin. There are many proteins that bind to cytoskeletons upon stretch[31], and it is likely that many rely upon exposure of buried binding sites. It is possible that the ~5 pN low force threshold that we have identified in talin, which corresponds to the force exerted by a single actomyosin contraction may be a common feature of other mechanosensitive adhesion proteins that couple to actin. Thus, the force-induced protein-protein interactions we observed in our studies might be a general mechanism that ensures that binding interactions only occur in the force range required to support physiological functions.

Methods

1. Hoffman, B. D. & Crocker, J. C. Cell mechanics: dissecting the physical responses of cells to force. *Annu. Rev. Biomed. Eng.* **11**, 259–88 (2009).
2. Bershadsky, A. D., Balaban, N. Q. & Geiger, B. Adhesion-dependent cell mechanosensitivity. *Annu. Rev. Cell Dev. Biol.* **19**, 677–95 (2003).
3. Humphries, J. D. et al. Vinculin controls focal adhesion formation by direct interactions with talin and actin. *J. Cell Biol.* **179**, 1043–57 (2007).
4. Carisey, A. et al. Vinculin regulates the recruitment and release of core focal adhesion proteins in a force-dependent manner. *Curr. Biol.* **23**, 271–81 (2013).

5. Hirata, H., Tatsumi, H., Lim, C. T. & Sokabe, M. Force-dependent vinculin binding to talin in live cells: a crucial step in anchoring the actin cytoskeleton to focal adhesions. *Am. J. Physiol. Cell Physiol.* **306**, C607–620 (2014).

6. Ciobanasu, C., Faivre, B. & Le Clainche, C. Actomyosin-dependent formation of the mechanosensitive talin-vinculin complex reinforces actin anchoring. *Nat. Commun.* **5**, 3095 (2014).

7. Elliott, P. R. *et al.* The Structure of the talin head reveals a novel extended conformation of the FERM domain. *Structure* **18**, 1289–99 (2010).

8. Anthis, N. J. *et al.* The structure of an integrin/talin complex reveals the basis of inside-out signal transduction. *EMBO J.* **28**, 3623–32 (2009).

9. Goult, B. T. *et al.* RIAM and vinculin binding to talin are mutually exclusive and regulate adhesion assembly and turnover. *J. Biol. Chem.* **288**, 8238–49 (2013).

10. Roberts, G. C. K. & Critchley, D. R. Structural and biophysical properties of the integrin-associated cytoskeletal protein talin. *Biophys. Rev.* **1**, 61–69 (2009).

11. Margadant, F. *et al.* Mechanotransduction in vivo by repeated talin stretch-relaxation events depends upon vinculin. *PLoS Biol.* **9**, e1001223 (2011).

12. Grashoff, C. *et al.* Measuring mechanical tension across vinculin reveals regulation of focal adhesion dynamics. *Nature* **466**, 263–6 (2010).

13. Vogel, V. & Hytönen, V. P. How force might activate talin's vinculin binding sites: SMD reveals a structural mechanism. *PLoS Comput. Biol.* **4**, e24 (2008).

14. Lee, S. E., Kamm, R. D. & Mofrad, M. R. K. Force-induced activation of talin and its possible role in focal adhesion mechanotransduction. *J. Biomech.* **40**, 2096–106 (2007).

15. Del Rio, A. *et al.* Stretching single talin rod molecules activates vinculin binding. *Science* **323**, 638–41 (2009).

16. Chen, H. *et al.* Improved high-force magnetic tweezers for stretching and refolding of proteins and short DNA. *Biophys. J.* **100**, 517–23 (2011).

17. Bois, P. R. J., O'Hara, B. P., Nietlispach, D., Kirkpatrick, J. & Izard, T. The vinculin binding sites of talin and alpha-actinin are sufficient to activate vinculin. *J. Biol. Chem.* **281**, 7228–36 (2006).

18. Wieprecht, T., Apostolov, O., Beyermann, M. & Seelig, J. Thermodynamics of the alpha-helix-coil transition of amphipathic peptides in a membrane environment: implications for the peptide-membrane binding equilibrium. *J. Mol. Biol.* **294**, 785–94 (1999).

19. Gao, Y. *et al.* Single reconstituted neuronal SNARE complexes zipper in three distinct stages. *Science* **337**, 1340–3 (2012).

20. Kishino, A. & Yanagida, T. Force measurements by micromanipulation of a single actin filament by glass needles. *Nature* **334**, 74–6 (1988).

21. Bois, P. R. J., Borgon, R. A., Vonrhein, C. & Izard, T. Structural dynamics of alpha-actinin-vinculin interactions. *Mol. Cell. Biol.* **25**, 6112–22 (2005).

22. Proszynski, T. J., Gingras, J., Valdez, G., Krzewski, K. & Sanes, J. R. Podosomes are present in a postsynaptic apparatus and participate in its maturation. *Proc. Natl. Acad. Sci. U. S. A.* **106**, 18373–18378 (2009).

23. Gingras, A. R. *et al.* The structure of the C-terminal actin-binding domain of talin. *EMBO J.* **27**, 458–69 (2008).

24. Han, J. *et al.* Reconstructing and deconstructing agonist-induced activation of integrin alphaIIbbeta3. *Curr. Biol.* **16**, 1796–806 (2006).

25. Lee, H.-S., Lim, C. J., Puzon-McLaughlin, W., Shattil, S. J. & Ginsberg, M. H. RIAM activates integrins by linking talin to ras GTPase membrane-targeting sequences. *J. Biol. Chem.* **284**, 5119–27 (2009).

26. Lee, H.-S., Anekal, P., Lim, C. J., Liu, C.-C. & Ginsberg, M. H. Two Modes of Integrin Activation Form a Binary Molecular Switch in Adhesion Maturation. *Mol. Biol. Cell* **24**, 1–22 (2013).

27. Sawada, Y. *et al.* Force sensing by mechanical extension of the Src family kinase substrate p130Cas. *Cell* **127**, 1015–26 (2006).

28. Ellis, S. J. *et al.* Talin autoinhibition is required for morphogenesis. *Curr. Biol.* **23**, 1825–33 (2013).

29. Goult, B. T. *et al.* Structural studies on full-length talin1 reveal a compact auto-inhibited dimer: implications for talin activation. *J. Struct. Biol.* **184**, 21–32 (2013).

30. Goksoy, E. *et al.* Structural basis for the autoinhibition of talin in regulating integrin activation. *Mol. Cell* **31**, 124–33 (2008).

31. Sawada, Y. & Sheetz, M. P. Force transduction by Triton cytoskeletons. *J. Cell Biol.* **156**, 609–15 (2002).

32. Banno, A. *et al.* Subcellular localization of talin is regulated by inter-domain interactions. *J. Biol. Chem.* **287**, 13799–812 (2012).

33. Fu, H. *et al.* Transition dynamics and selection of the distinct S-DNA and strand unpeeling modes of double helix overstretching. *Nucleic Acids Res.* **39**, 3473–81 (2011).

34. Chen, H. *et al.* Mechanical perturbation of filamin A immunoglobulin repeats 20-21 reveals potential non-equilibrium mechanochemical partner binding function. *Sci. Rep.* **3**, 1642 (2013).

35. Chen, H. *et al.* Differential mechanical stability of filamin A rod segments. *Biophys. J.* **101**, 1231–7 (2011).

Acknowledgments

Author contributions

J.Y. and M.P.S. designed the research and supervised the experiments. M.Y. performed the experiments. M.Y., B.T.G., J.Y., H.C. and P.C. interpreted and analyzed the data. H.C. built the tweezers for the experiments. M.Y., B.T.G., J.Y. and M.P.S. wrote the paper.

Additional information